How does Wi-Fi 6 fare? An industrial outdoor robotic scenario

Mina Rady, Oana Iova, Hervé Rivano, Angeliki Deligianni, Leonidas Drikos

Ad Hoc Networks 156 (2024) 103418

Contents lists available at ScienceDirect

Ad Hoc Networks

journal homepage: www.elsevier.com/locate/adhoc

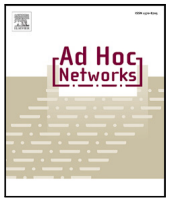

How does Wi-Fi 6 fare? An industrial outdoor robotic scenario

Mina Rady [a,b,*], Oana Iova [a], Hervé Rivano [a], Angeliki Deligianni [c], Leonidas Drikos [c]

[a] Univ Lyon, INSA Lyon, Inria, CITI, EA3720, 69621 Villeurbanne, France
[b] Université Paris-Saclay, CEA, List, F-91191, Palaiseau, France
[c] Glafcos Marine Ltd., Piraeus, 18537, Greece

ARTICLE INFO

Keywords:
Wi-Fi
IEEE 802.11
Industrial networks
Robotics
PTP
ROS

ABSTRACT

Wi-Fi is a standard off-the-shelf solution for industrial robotics. The IEEE 802.11ax amendment extends it to support the 6 GHz band, 160 MHz bandwidth and bit-rates up to 9.6 Gbps. In this article, we evaluate the performance of Wi-Fi 6 compared to Wi-Fi 5 and Wi-Fi 4. We select 9 physical layers (PHYs) representing different Wi-Fi generations and we evaluate their performance in an industrial shipyard in the presence of high radio frequency interference and metallic obstructions. We deploy setup of a robotic station (STA) and a controller STA with three applications running in parallel: a robotic STA is sending a high throughput stream to a controller, a Robotic Operating System (ROS) application is sending time-critical control commands to the robotic STA, Precision Time Protocol (PTP) keeps synchronizing the clocks between both STAs. We evaluate the performance in terms of three Key Performance Indicators (KPIs): streaming throughput, IP-level delay using PTP, and Application-level delay of ROS control packets. The networks are run in: Short range Line of Sight (LoS), Medium range LoS, Long range None-LoS (NLoS), and Long range mixed settings. We note that depending on the PHY configuration, an older Wi-Fi generation may outperform Wi-Fi 6. We further observe trade-offs between the different PHYs: wide channel PHYs (e.g. 160 MHz) had best throughput reaching up to 900 Mbps while PHYs while 80 MHz or 20 MHz bandwidth achieved as low as 9 ms delay. This motivates further research in multi-PHY adaptation for KPIs specific to industrial robotics.

1. Introduction

Industrial automation has been empowered by the advances in use of robotics and wireless networks. The use of robots helps speed up tasks, get easy access to crowded spaces, and diminish the risk of injuries for people. Robots may execute tasks autonomously or under the command of a human teleoperator, after analyzing divers data collected from sensors. To collect all the data from the robots, a communication network has to be put in place, and considering the free-movement of the robots, wireless technologies are preferred.

As a concrete example, industrial robotics emerged as a promising solution for ship inspections in the maritime industry [1], owing to the complexity of ships and the unpredictable environments in which they operate [2,3]. Current methods involve full visual inspections conducted by divers or certified individuals on a dry dock, utilizing costly and time-consuming scaffolding or cherry pickers [4]. These methods can risk human health and safety as they result into fatigue, accidents, and oversights [4,5]. In contrast, robotics offer higher efficiency, accuracy, and cost-effectiveness [1,6].

From a technical standpoint, efficient robotic inspections involve a swarm of drones and crawlers that collect the inspection data (e.g., video feeds). To avoid time and cost consuming post-inspection processes, the captured data should be live streamed wirelessly to a remote analysis server, which is throughput intensive. For securing necessary legal approvals to conduct inspections using a robot swarm, the network also needs to comply to safety and real-time requirements for the standard inspection process and deliver with real-time constraints delay sensitive data. These critical packets are both upstream, e.g., locations or images that are used for obstacle and defect detection, and downstream, e.g., drones control packets for mission control or collision avoidance when obstacle detection algorithms are offloaded to a remote server [7–9].

Ensuring such network metrics, called Key Performance Indicators (KPIs), for wireless connectivity in industrial outdoor sites is still an open question and a growing area of interest, even outside robotic applications. The harsh environment in an industrial site, even outdoor, is very challenging for radio waves due to: (i) metallic obstruction from mechanical equipment, (ii) presence of large bodies of water (or other liquids) that increase radio signal attenuation, and (iii) interference from external wireless sources.

* Corresponding author at: Université Paris-Saclay, CEA, List, F-91191, Palaiseau, France.
E-mail address: mina.rady@cea.fr (M. Rady).

https://doi.org/10.1016/j.adhoc.2024.103418
Received 27 September 2023; Received in revised form 20 December 2023; Accepted 21 January 2024
Available online 23 January 2024

The IEEE 802.11 standard, commercially known as Wi-Fi, represents one of the most commonly used commercial off-the-shelf (COTS) solutions for robotic application due to the maturity of the standard and to the wide range of available Wi-Fi network interface cards (NICs). Wi-Fi has evolved to support a wide diversity of physical layer (PHY) configurations such as several frequency bands (2.4 GHz, 5 GHz, and 6 GHz), and channel bandwidths (20, 40, 80, and 160 MHz). From one version to another, several features have been added, enabling the latest version, Wi-Fi 6, to reach bit-rates up to 9.6 Gbps. However, as more and more configurations are possible, finding the best one for a specific environment that would respect the KPIs of the application, is still an open challenge. The questions that we try to answer in this paper are:

How does Wi-Fi 6 fare in an industrial outdoor scenario for a robotic application? Is there a specific configuration that fulfills all the KPIs of the application?

We address these questions by running an exhaustive experimental campaign in an industrial shipyard. We evaluate the performance of Wi-Fi 6 against the previous generations of Wi-Fi (4 and 5) at different locations in the shipyard, using different PHY configurations. The experimental campaign provides a realistic performance evaluation, which is commonly used in wireless networks benchmarking in the research community (e.g., [10–12]).

Specifically, the contribution of this paper is three-fold:

1. We evaluate the performance of a total of nine PHY configurations of Wi-Fi 4, 5 and 6, in four locations mixing different distances and line of sight conditions.
2. Out of all the Wi-Fi configurations tested, we show that the 6 GHz and 5 GHz frequency bands had better performance than the 2.4 GHz band, and that wide channels yield higher streaming throughput, while narrow channels yield lower delay for control traffic.
3. We show that there is no configuration that is best for all KPIs in all locations.

The rest of this paper is organized as follows. Section 2 provides an overview of the IEEE 802.11 standard, Wi-Fi performance evaluation, and related industrial wireless networks. Section 3 introduces the experimental setup and KPIs used for the experimental campaigns. Section 4 presents the experimental results. Finally, Section 6 presents a summary of the observations, learned lessons, and future work.

2. Related work

We start this section by presenting an overview of the IEEE 802.11 standard [13] and its variations in Section 2.1. We then present the related work in the performance evaluation of Wi-Fi networks in Section 2.2. Finally, we present related work on existing protocols used for industrial applications in Section 2.3.

2.1. An overview of the IEEE 802.11 standard

Wi-Fi networks implement different versions of the IEEE 802.11 standard. At the PHY layer, early amendments of the IEEE 802.11 standard defined bit-rates between 1 Mbps and 4.5 Mbps in the 2.4 GHz RF band. The IEEE 802.11b amendment introduced bit-rates up to 11 Mbps in the 2.4 GHz band. Simultaneously, The IEEE 802.11a amendment included bit-rates up to 54 Mbps using the orthogonal frequency division multiplexing (OFDM) modulation in the 5 GHz band. Later key amendments: IEEE 802.11g, IEEE 802.11n (commercially known as Wi-Fi 4), IEEE 802.11ac (commercially known as Wi-Fi 5), and IEEE 802.11ax (commercially known as Wi-Fi 6) included faster bit-rates. The latest IEEE 802.11ax amendment (2020) includes bit-rates up to 9.6 Gbps using 1024-Quadrature Amplitude Modulation (QAM) based OFDM [14]. These bit-rates are achieved using (mainly) three factors: (1) increased symbol rate by using denser QAM constellations in OFDM, (2) adopting multiple-input–multiple-output (MIMO) antennas to enable parallel transmit/received paths (introduced in the IEEE 802.11n amendment), and (3) increasing channel bandwidth (BW) from 20 MHz up to 40, 80, and 160 MHz BW.

At the medium access control (MAC) layer, IEEE 802.11 uses carrier sense multiple access with collision avoidance (CSMA/CA) [13]. CSMA/CA is a non-deterministic MAC layer using a random back-off counter to mitigate collisions using the Hybrid Coordination Function [13]. The standard defines four Quality of Service(QoS) access categories: voice, video, best effort, and background.

The IEEE 802.11ax amendment introduced an essential improvement to the MAC layer, as highlighted by Khorov et al. [15]. As IEEE 802.11 deployments have increased in density (e.g., in malls, airports etc.) a purely none-deterministic MAC based on CSMA/CA is challenged when hundreds of Access Points (APs) coexist [15]. At the MAC layer, IEEE 802.11ax introduces orthogonal frequency division multiple access (OFDMA) on top of CSMA/CA. Time and frequency resources are divided into resource units, and stations (STAs) request to be allocated dedicated contention-free resource units for their transmissions. This way, they are guaranteed to not interfere with neighboring STAs running the same mechanism. It also allows parallel time-synchronized multi-stream and multi-user transmissions using the full capacity of the MIMO antennas [15].

Further improvements are expected in the IEEE 802.11be amendment (i.e., Wi-Fi 7) [16]. Specifically, preamble puncturing is proposed to make use of underutilized channel resources by allowing more flexible channel resource sharing between STAs. For example, a transmission on an 80 MHz channel can use partially resources from a 20 MHz channel. Also, multi-link operation is proposed to allow concurrent transmissions within the same band or across different bands. Such features are expected to improve network latency by better exploitation of available frequency resources.

At the MAC layer, a rate adaptation algorithm (RAA) selects the PHY bit-rate to be used based on link quality. The RAA is outside of the scope of the IEEE 802.11 standard and it is left to vendor implementation (Sec. 10.7 in [13]). The large number of the available PHYs poses a challenge for the RAA for efficient and stable PHY adaptation [15]. Sammour et al. [17] classify RAAs into three categories: (1) Explicit Feedback RAAs, which are receiver-driven algorithms where the rate decision is based on the receiver and relayed to the sender piggybacked on control frames, (2) Implicit Feedback RAAs, which are sender-driven algorithms where the sender decides on the rate based on the metrics observed from its end such as Packet Error Rate (PER) or Frame Loss Rate (FLR), and (3) Hybrid RAAs, where the algorithm combines sender and receiver feedback for the rate decision making.

Minstrel [18] is one of the commonly adopted RAAs that is implemented in the recent drivers of wireless NICs such as the `Intel AX211` and `Atheros Ath9k` NICs. It is an Implicit Feedback algorithm that relies on FLR metric for decision making [17]. During a sampling period, it evaluates randomly selected bit-rates, favoring high-throughput PHYs. Afterwards, it selects the first and second highest throughput bit-rates and the bit-rates with the highest probability of success. It maintains the history of FLR for used bit-rates and it is approximated using Exponentially Weighted Moving Average [19].

2.2. IEEE 802.11 performance evaluation

Recent articles evaluate performance of IEEE 802.11 networks. Muhammad et al. evaluate the performance of IEEE 802.11ac and IEEE 802.11ax using different channel BW [20]. The authors run uplink and downlink streams between a STA and an AP with and they report the performance results as a function of the link signal-to-noise ratio (SNR). They observe that the throughput of the IEEE 802.11ax network is saturated at the same rate using 80 and 160 MHz BW and that the

network does not benefit from doubling the BW. Authors attribute this to hardware implementation.

Frommel et al. evaluate the performance of collocated IEEE 802.11ax and IEEE 802.11n networks in the 5 GHz band [21]. Authors use simulations and experimental setup in a lab environment. They observe that IEEE 802.11ax has a 60% throughput increase with respect to IEEE 802.11n, reaching a maximum of 225 Mbps. The IEEE 802.11n network reaches throughput superior or similar to the IEEE 802.11ax network in several runs, both in simulation and experimentally.

Tramarin et al. study the reliability of IEEE 802.11 networks for industrial applications and they test how different RAAs react to decreased link quality [22]. They test RAAs in IEEE 802.11n and they demonstrate that, depending on the type of the RAA, the used bit-rate can drop instantaneously, or slowly, or fluctuate, before it stabilizes. In case of instantaneous bit-rate drops or fluctuations, frame loss and delay are severely impacted.

Finally, Hayat et al. compare the performance of the IEEE 802.11n and IEEE 802.11ac networks in mobility and they demonstrate the evolution of bit-rate and throughput as a the distance between the STA and the AP increases using drones as STAs [23]. Authors find that at distances <50 m the IEEE 802.11ac link is 50% higher in throughput despite using 200% faster bit-rate. In distances >50 m, both networks maintained the same throughput.

Articles in this section provide significant experimental evaluation of Wi-Fi throughput in different conditions. This paper goes a step further by evaluating the performance of the nine different Wi-Fi configurations in an industrial setup for robotics use-case.

2.3. Evaluation of industrial wireless networks

Industrial wireless networking is an evolving domain of research and standardization. Using the RF medium brings challenges for reliability and latency required for industrial networks, such as: interference from external networks, channel variations, and multi-path fading. To ease the deployment of industrial robotic networks, the implementation of several protocols is needed, such as the Precision Time Protocol (PTP) and the Real-time Publish Subscribe (RTPS) Wire Protocol.

The Precision Time Protocol (PTP) defined by the IEEE 1588 standard [24] was designed to enable micro-second scale time synchronization for Ethernet networks. Today, it is also used in Wi-Fi networks and in robotic applications. In a network with PTP deployment, a Grand Master (GM) clock source is defined. Other nodes in the network can be set as slaves to synchronize to the GM or a negotiation process can take place for the network to elect the GM. The GM estimates the transmission time offset with the slave nodes using pairs of `Sync` and `Follow Up` requests. A slave node tracks the GM clock using periodic `Delay Request/Delay Response` exchanges with the GM. PTP messages are encapsulated with User Datagram Protocol (UDP) over Internet Protocol (IP).

Seijo et al. [25] evaluate PTP synchronization accuracy under different channel conditions. They emulate IEEE 802.11g channel with 20 MHz BW in the 2.4 GHz band using a hardware channel emulator. They achieve synchronization offset under 200 ns using hardware timestamping from an open software-defined radio architecture. They show that varying channel conditions such as Doppler shifts and multi-path fading decreases synchronization accuracy.

Thi et al. [26] evaluate PTP delay and synchronization accuracy in Wi-Fi networks in a lab setup. Software timestamping is used as would be expected with COTS equipment. The experiment shows a delay under 100 ms over the Wi-Fi link compared to 40 μs over the Ethernet link.

Sudhakaran et al. [27] evaluate the performance of an industrial network in a collaborative robotic workcell. Authors enable PTP synchronization in addition to the TSN IEEE 802.1Qbv Ethernet standard on top of a Wi-Fi network. They evaluate the 20 MHz BW channel using different PHY bit-rates. Experiments demonstrate an improvement of 10%–30% in the ratio of packets delivered within delay of <5 ms when TSN is enabled.

Real-time Publish Subscribe (RTPS) standard is another protocol used in industrial networking. It is defined by the Object Management Group (OMG) [28] as an interoperability protocol for the OMG Data Distribution Service (DDS) [29]. Messages are published under declared topics that reach nodes subscribed to the topic. RTPS is used by DDS to create seamless exchange between components of robotic or vehicular networks. DDS [29] is a data-centric platform that defines QoS categories to tune RTPS performance for robotic data exchanges. For example, *Recency* category keeps track of the latest reading of a data value and in case of packet loss, it only sends the latest reading while discarding older readings. DDS over RTPS has been adopted as the standard communication interface for ROS [30]. ROS provides a framework to integrate and control complex robotic and vehicular systems. It relies on DDS to discover available communications interfaces per each system and to manage data transfer locally or across the network.

Pandey et al. [31], evaluate Wi-Fi network quality for a robot in mobility. Authors evaluate the 2.4 GHz and 5 GHz bands in different topologies using an IEEE 802.11ac network. The experiment is conducted in a lab setting using Robotic Operating System (ROS) streaming and control setup. They observe throughput up to 70 Mbps and delay down to 63 Mbps using the 5 GHz band.

Performance of industrial networks has been evaluated according to typical KPIs: latency, packet loss, and throughput. However, performance of industrial *robotic wireless* networks calls for a distinct KPI that reflects the impact of the lossy network on robotic (swarm) behavior. Recent research by Abu-Aisheh et al. showed that lossy communications can impact the time to finish the exploration task of a swarm for micro-robots [32]. Packets carrying critical information such as control commands or real-time location need a reliable flow in a timely manner. Excessive delays for these packets undermines the efficiency of the robot operation, the safety of the deployment, and the usability by the human teleoperator. Former research by MacKenzie et al. studied the impact of control latency on the performance of the human teleoperator. Their experiments on human subjects showed that their performance errors began to increase noticeably with control delays larger than 75 ms [33,34]

The surveyed research in this section shows an increasing maturity in industrial wireless networking. Research on PTP evaluation over Wi-Fi presented in [25–27] considers one band and channel BW for their experiments. This article goes a step further by considering the impact of the PHY configuration in terms bit-rate, band, and channel BW on the defined KPIs. We provide an exhaustive range testing campaign in a real industrial setup in a standard robotic scenario involving streaming, control, and synchronization simultaneously.

3. Experimental setup and methodology

To see how Wi-Fi 6 fares with respect to the other Wi-Fi versions in an industrial robotics setting, we conduct experimental campaigns in different scenarios and with different PHY configurations. In this section, we provide an overview of the context and methodology of the experimental campaign. We introduce an overview of the industrial site and selected testing locations in Section 3.1. We provide the architecture of the experimental setup and the details on how the data is collected and processed in Section 3.2. Then we introduce in Section 3.3 the KPIs used to evaluate the end-to-end network performance.

3.1. Experimental site

We chose the Perama shipyard [35] as our experimental site, as it is a major industrial hub for construction and maintenance of large

Fig. 1. Satellite view of the location used for experiments in Perama Shipyard, Piraeus, Greece.
Source: Google Earth.

freighters and yacht-vessels in Piraeus, Greece. The shipyard has a surface area of 26,000 m^2 and has mechanical and electrical workshops that perform constructions, repairs and maintenance related to mechanical and steel components of vessels. The platform is densely occupied by large metallic structures such as containers, cranes, forklifts, and cherry pickers. The area is replete with steel welding facilities that operate on large structures, such as ship hulls or extensive metallic frameworks. These structures take up a significant amount of space and are often tightly packed together, creating a dense metallic environment.

In order to have a realistic setup, we placed the Wi-Fi access point (AP) on a high point (at 8 m) in a location close to the docks, as illustrated in Fig. 1. The locations of the stations (STA) were then chosen such that they provide different conditions and challenges for the wireless link in terms of: range, RF interference, and physical obstructions. More precisely:

1. **Short range LoS.** Location 1 was chosen at 13 m away from the AP, characteristic to short-range communications without any obstacles, i.e., line-of-sight (LoS) conditions.
2. **Medium range LoS.** Location 2 was chosen at 60 m away from the AP, characteristic to medium-range communications, close to several buildings, but still in LoS of the AP.
3. **Long range NLoS.** Location 3 was chosen at 130 m away from the AP, on the dock (Fig. 2). This location is characteristic to long-distance communications with obstacles, i.e., no line-of-sight (NLoS) conditions, situated in a complex environment: across a large building (with respect to the AP), close to the water and in the presence of an array of ships.
4. **Long range mixed**. Location 4 was chosen at 150 m away from the AP, with multiple metallic obstructions present on the ground between the STA and the AP (such as cherry picker lifts, containers, and cylindrical tanks) (Fig. 3). Considering the height of the AP (8 m), this setup results in a mixed LoS and NLoS conditions. This location is characteristic to long-distance communications with partial metallic obstructions common in industrial environments.

We choose to make the experiment in such a realistic setup to push the Wi-Fi network to its limits. We test the network in four different scenarios to observe the common and different patterns across all scenarios. We believe that the presence of realistic challenges brings insights that are different from tests done in an ideal RF environment.

A shipyard is an extremely challenging environment for wireless communications due to the presence of metallic structures, ships, mobile vehicles, humans, and water, each of them impacting differently the propagation of radio waves. This leads to network performance degradation due to interference from existing Wi-Fi networks, such as personal printers and smartphone hot-spots, networks deployed in surrounding construction, repair sites and on the docked vessels.

Indeed, a scan of the existing Wi-Fi networks performed at the experimental site showed a varying and dense radio channel occupation in the 2.4 GHz and 5 GHz frequency bands, as can be seen in Figs. 4 and 5. Particularly, we observe that in location 3 (Fig. 2), both 2.4 GHz and 5 GHz frequency bands present very high channel activity due to the presence of 30 co-located networks causing severe channel interference. Considering the 6 GHz frequency band, our Wi-Fi network was the only one deployed on the site.

3.2. Experimental setup

We consider the general case of remotely operated robots in an industrial environment. In such a use case, a robot is streaming data including camera images and sensors data (e.g., Light Detection and Ranging scanner or ultrasound sensor). The controller (machine or human) analyzes the received data and sends control commands to the robot. The robot communicates with the controller over Wi-Fi. Our goal here is to evaluate Wi-Fi 6 against different Wi-Fi standards and configurations in a realistic industrial scenario for this type of communication.

Hardware and software. We prepared an architecture that is typical to a robotic setup as illustrated in Fig. 6. The Wi-Fi connectivity is ensured on site by an Asus AX-GTE11000 AP [36]. The robot is represented by a laptop that uses an `Intel AX211` NIC for its Wi-Fi connectivity. The controller is also represented by a laptop, and it communicates with the AP via GbE. Both laptops run ROS 2 [30] over Linux Ubuntu OS and implement PTP [37] and `iPerf` [38] (see Fig. 7).

We use three types of traffic: (1) time synchronization and delay measurement traffic, (2) high-bandwidth TCP stream to mimic sensor and video streaming from the robot in uplink, and (3) downlink UDP packets to mimic control commands to the robot[1] :.

PTP synchronization is enabled on both computers, allowing us to measure the single-trip delay between them. As outlined in the

[1] The equipment we used had no per flow QoS configuration capability (as it often the case with commercial off-the-shelve products). We presume, but cannot confirm, that, by default, the AP treats UDP and TCP streams with the same Best Effort QoS category. Therefore, it would be an interesting future work to evaluate the impact of such configurations.

Fig. 2. Location 3 at the dock in the presence of an array of ships.

Fig. 3. Location 4 surrounded by metallic obstructions, typical of industrial environments.

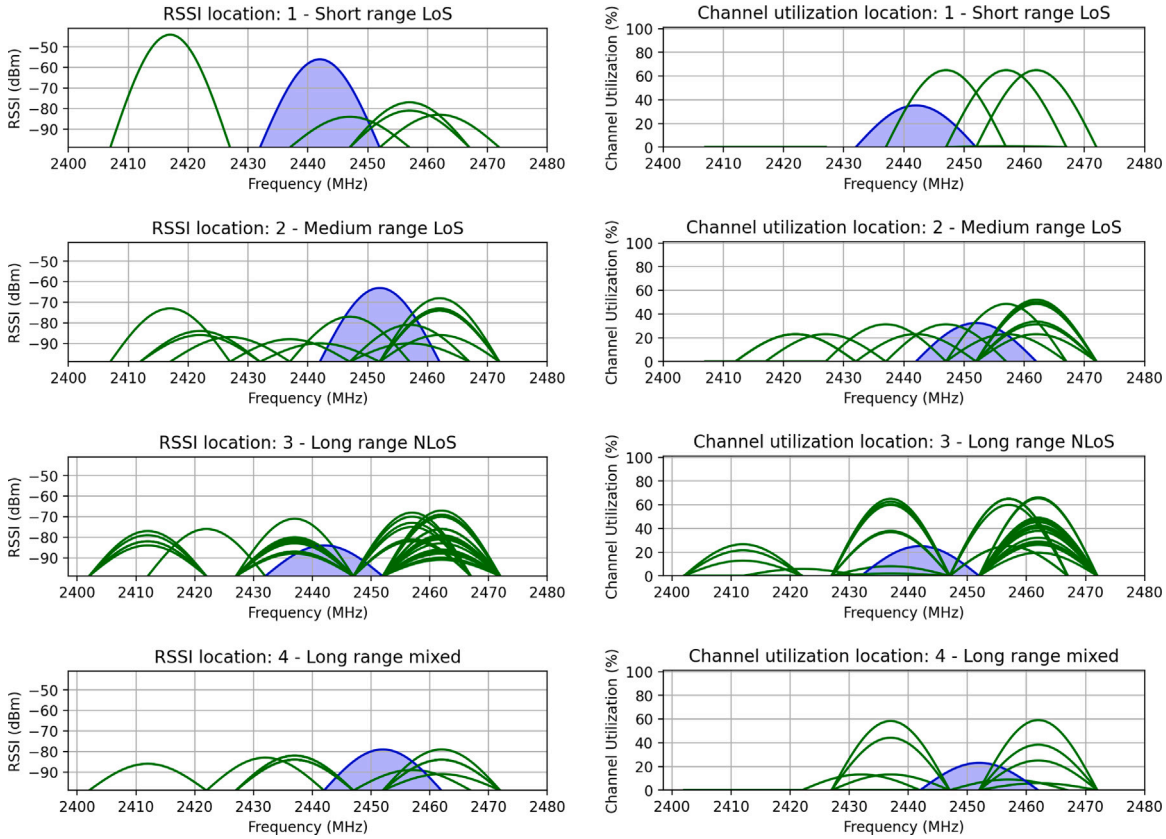

Fig. 4. Plot of the RSSI (left) and channel utilization (right) of the APs in the 2.4 GHz band. We highlight the presence of our network in *blue*. The shipyard is a noisy RF environment specially in location 3 near the ships. Samples of the channel utilization indicate that the APs are in fact active.

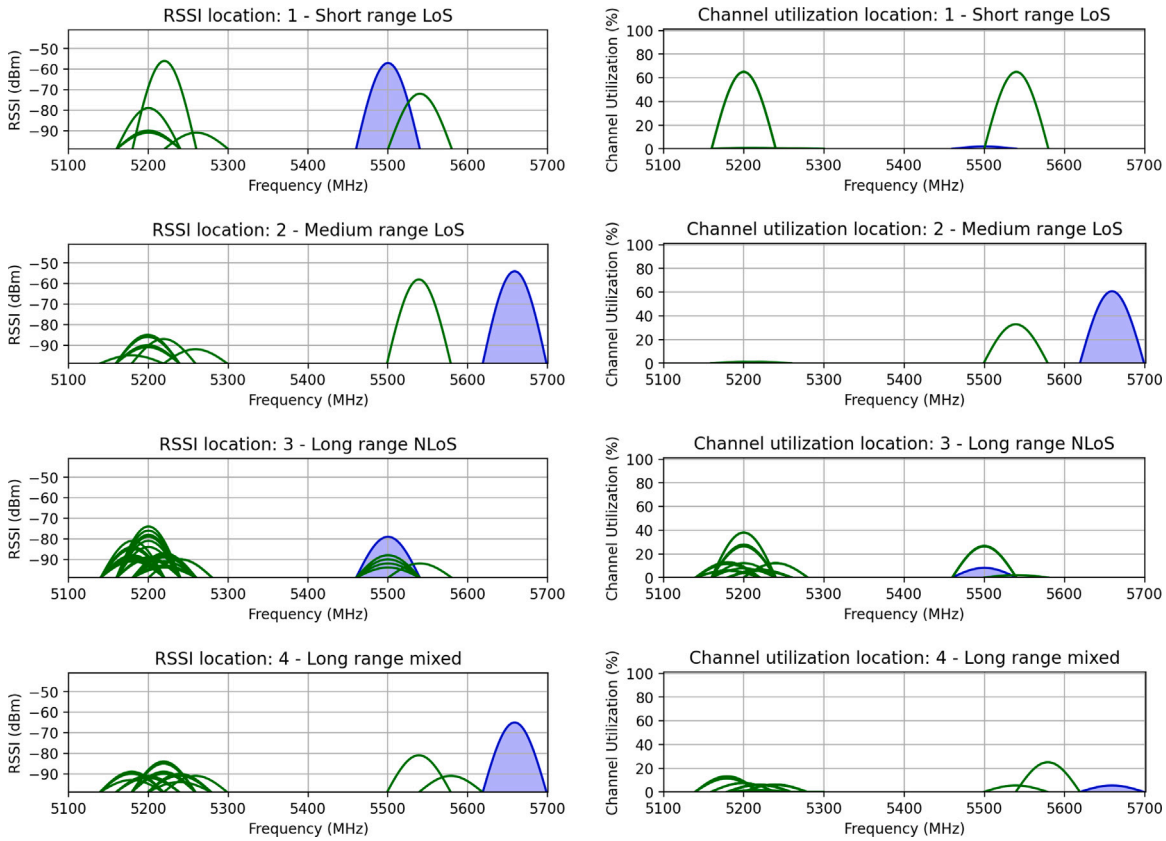

Fig. 5. Plot of the RSSI (left) and channel utilization (right) of the APs in the 5 GHz band. We highlight the presence of our network in *blue*. The 5 GHz band was significantly less occupied, however it was still active at the harbor in the vicinity of the ships.

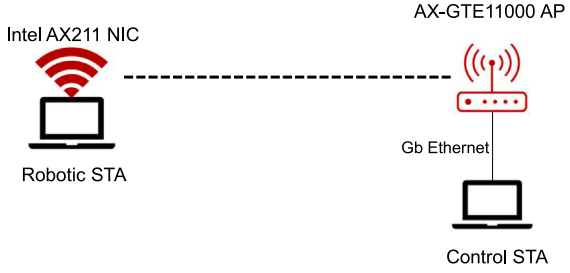

Fig. 6. Architecture of the network used in the experiment with hardware details.

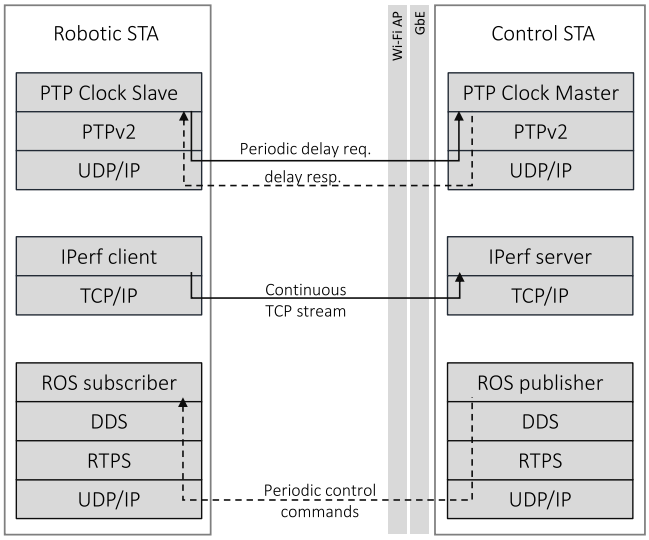

Fig. 7. Software view of the experimental setup: the robotic STA continuously streams data to the controller STA using `iPerf`, while the controller periodically sends commands to the robot through ROS. PTP is used for computing the delay between the two STAs.

standard [24], the PTP slave (on the robotic STA in our setup) sends periodic requests at 1 Hz interval to the master (on the controller STA in our setup) requesting the difference between their clocks. The master calculates the difference in clocks and responds with instructions to the slave including the necessary correction to its clock. Then the slave uses this information to update its local clock and synchronize to the master. Messages carrying the timestamps from sender to receiver are sent using UDP/IP protocol stack.

We use `iPerf` [38] to generate a TCP stream from the robotic STA to the controller STA. It uses the standard Cubic congestion control algorithm [39] to reach maximum achievable application throughput. `iPerf` is configured to reach a target BW of 1 Gbps since the AP is connected to the controller via a GbE link. This allows us to capture the maximum achievable end-to-end streaming throughput in each scenario.

Finally, we created a ROS 2 application [30] using a publish/subscribe messaging interface similar to the control traffic that is sent from the controller STA to the robotic STA. The controller STA sends a control packet every 500 ms mimicking a classical periodic control loop used in robotic applications. Each control packet payload consists of a sequence number and an application timestamp. At the reception of the control packet, the robotic STA logs it and appends to it the application received timestamp and the location of the robotic STA.

Wi-Fi settings. We compared Wi-Fi 6 against Wi-Fi 4 and 5 by testing the performance of a total of nine configurations representing a

Table 1
The Wi-Fi configurations used in our experiments ordered by maximum bit-rate.

802.11 amendment	Wi-Fi version	RF band	Channel BW	Maximum bit-rate	Acronym
802.11ax	Wi-Fi 6E	6 GHz	160 MHz	1254 Mbps	ax/6/160
802.11ax	Wi-Fi 6	5 GHz	80 MHz	1201 Mbps	ax/5/80
802.11ac	Wi-Fi 5	5 GHz	80 MHz	1201 Mbps	ac/5/80
802.11ax	Wi-Fi 6E	6 GHz	80 MHz	865 Mbps	ax/6/80
802.11ax	Wi-Fi 6	2.4 GHz	20 MHz	287 Mbps	ax/2.4/20
802.11ax	Wi-Fi 6	5 GHz	20 MHz	287 Mbps	ax/5/20
802.11ac	Wi-Fi 5	5 GHz	20 MHz	287 Mbps	ac/5/20
802.11ax	Wi-Fi 6E	6 GHz	20 MHz	229 Mbps	ax/6/20
802.11n	Wi-Fi 4	2.4 GHz	20 MHz	144 Mbps	n/2.4/20

range of maximum PHY bit-rates between 144 Mbps and 1.25 Gbps as listed in Table 1. We conducted tests in the three available frequency bands: 2.4 GHz, 5 GHz, and 6 GHz. We also test three different channel bandwidths: 20 MHz (narrow), 80 MHz (in-between), and 160 MHz (wide). We enabled automatic channel selection in the AP, which is a separate mechanism from the Wi-Fi generation and the rate adaptation algorithm, to select channel least used by surrounding APs. For conciseness, we will refer to each parameter configuration in an acronym that includes three key information: *Wi-Fi generation/frequency band/bandwidth*. For example, ax/5/80 represents IEEE 802.11ax (Wi-Fi 6) in the 5 GHz band with a bandwidth of 80 MHz.

We run each of the 9 configurations in each of the 4 locations for 180 s. Considering how difficult it is to obtain access to an industrial facility for a sufficiently long period of time to conduct such experiments, we made available online both the source code for the scripts used in the experiment as well as the collected data.[2]

3.3. Key performance indicators

As previously mentioned, we consider the general case of remotely operated robots in an industrial environment, where a robot is streaming data and a controller analyses the received data and sends control commands to the robot. In this scenario, we identify four KPIs that we used to evaluate the aforementioned Wi-Fi configurations in an industrial outdoor robotic scenario:

1. **Streaming throughput.** Considering the large data that has to be sent from the robot to the controller, the end-to-end streaming throughput is an important KPI. We used `iPerf` to generate a TCP stream from the robotic STA to the controller (as explained in Section 3.2). We log the achieved throughput at 1 s intervals to consider its evolution throughout the experiment.
2. **PTP delay.** This KPI is essential to time-sensitive localization and coordination of robotic swarm missions, as it impacts the clock synchronization accuracy. The PTP delay measures the single-trip delay between the robotic STA and the controller STA and it reflects the latency of the wireless network including MAC-layer re-transmissions.
3. **ROS control packets delay.** Considering the time-sensitive nature of the ROS control traffic sent to the robots, it is important to also measure their delay. In this case, ROS messages carrying the timestamps from sender to receiver are sent over the DDS/RTPS/UDP/IP protocol stack using the DDS QoS features outlined in Section 2.3.
4. **ROS control packets Constrained Delay Ratio (CDR).** If time critical packets are excessively delayed, it will take a longer time to finish a given task. Hence, a network has to avoid excessive delays. For example, a network where 100% the packets were delivered under 75 ms is preferred to a network where 90% of the packets are delivered under 10 ms while the other 10% are delivered above 75 ms. CDR measures the ratio of control packets with latency under the 75 ms threshold necessary for seamless human operator experience, as introduced by previous research in Section 2.3.

We present in the following section the experimental evaluation of these KPIs for each Wi-Fi configuration in all scenarios.

4. Results

In this section, we present the performance results of the different Wi-Fi standards and configuration in all the measuring points in terms of above mentioned KPIs: streaming throughput (Section 4.1), PTP and ROS control packets delay (Section 4.2), and ROS control packets Constrained Delay Ratio (Section 4.3). We highlight the best performing configuration and the performance trade-offs in each scenario and each KPI in Section 4.4.

4.1. Streaming throughput

We plot the cumulative density function (CDF) of the streaming throughput achieved with each configuration in all locations in Fig. 8. The first thing that we notice is that Wi-Fi 6 in the 6 GHz band maintained the highest throughput in all the locations. More specifically, the ax/6/160 for the Short range LoS, Medium range LoS, and Long range NLoS scenarios, and ax/6/80 for the Long range mixed scenario. The highest throughput of ≈900 mbps was achieved at Short range LoS scenario using ax/6/160 network. This can be explained by the gain in throughput using the wide 160 MHz channel. However, at the Long range mixed scenario, the 80 MHz channel outperformed the 160 MHz channel as the ax/6/80 configuration reached 250 mbps. This can be attributed to the receiver sensitivity of the 80 MHz channel that is lower than the 160 MHz channel as described in the IEEE 802.11 standard Table 21-25.

We note that the throughput of the IEEE 802.11ax (Wi-Fi 6) network was not always better than the older IEEE 802.11ac or IEEE 802.11n networks. For instance, we observe in Long range NLoS scenario that the ac/5/80 configuration outperforms the ax/5/80 scenario by 20 Mbps. We observed that the AP had selected a channel that overlapped with interfering APs during the ax/5/80 run in this location. Although Wi-Fi-6 is intended to improve performance in dense networks, it was still impacted in the presence of external interference, compared to the Wi-Fi-5 network of the same channel configuration. Therefore, the choice of frequency and channel BW has the most impact on link performance, throughout the Wi-Fi standard generations.

4.2. Delay

In this section, we measure the PTP delay and we compare it to the delay of ROS control application messages as described in Fig. 7.

Fig. 9 shows the CDF plot of PTP delay at steady state after 120 s into the experiment, which leaves PTP the time to synchronize the slave and master clocks. The best delay performance in Short range LoS, and Medium range LoS scenarios was achieved using ax/6/80 network with

[2] https://github.com/minarady1/wifi_for_industrial_robotics.

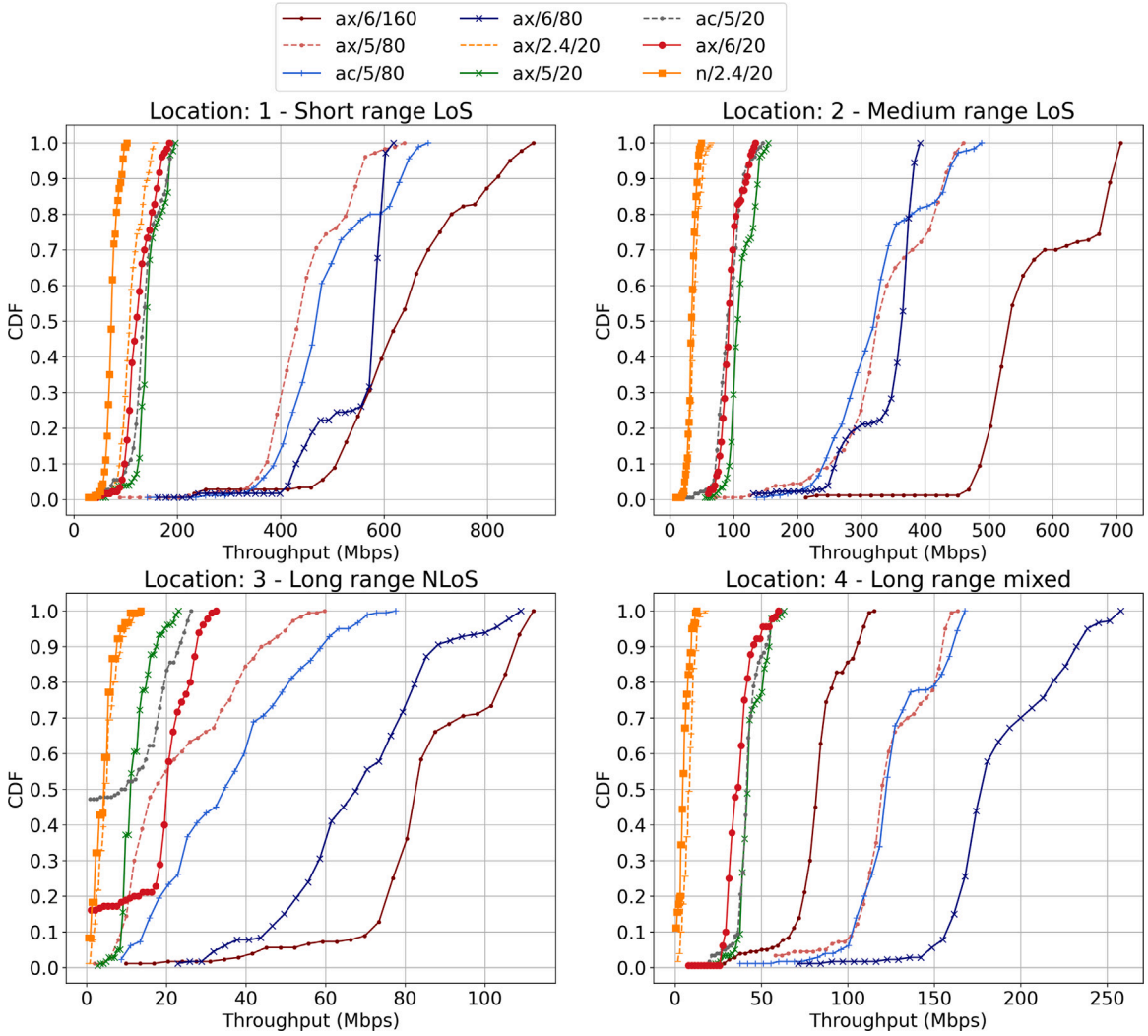

Fig. 8. Achieved streaming throughput of each Wi-Fi configuration in the four locations.

delay ≈10 ms and ≈12 ms respectively. In the Long range NLoS scenario, the best delay was achieved by the ax/5/20 network. In the Long range mixed scenario, ax/5/80 network offers the best delay.

We note that all best configurations belong to the 5 GHz or 6 GHz bands. This is surprising because, although the ax/6/160 outperformed others in 3 scenarios in terms of throughput KPI, it is not the case for delay. This can be attributed to the fact that the ax/6/160 has the highest receiver sensitivity among all other configurations. Therefore, it incurs higher frame loss than other configurations, triggering more re-transmissions, even if its overall throughput is higher. We discuss this in more detail in Section 5.

We note that the Wi-Fi 6 configurations are not always better than older generations. For instance, in the Short range LoS scenario, the ax/2.4/20 configuration had median delay of ≈17 ms compared to the IEEE 802.11n network that had a median delay of ≈11 ms. We noted from the logged data that the AP had selected channel the overlapped with another external AP during the run of the ax/2.4/20 network. Similarly, the ax/2.4/20 network suffered the same delay degradation as the n/2.4/20 network in Long range NLoS scenario. We observe dense Wi-Fi deployments, spanning all channels, around this location as seen in AP scans in Fig. 4. Surrounding APs had both high RSSI and high channel utilization which challenge the reliability of the link. Thus, the ax/2.4/20 network was still vulnerable to external interference which led to an increase in delay due to resulting re-transmissions. We choose to report these results even it is influenced by an overlapping channel as it represents the reality faced by Wi-Fi networks in an industrial setup.

Clock synchronization offset is important to functions like robotic swarm coordination or localization. We show in Fig. 10, the measured clock offset between the STA and the controller using PTP. We select the best performing configurations in the four scenarios and we observe that the clocks were most tightly synchronized using the 80 MHz channel of Wi-Fi in the less challenging scenarios (Short range LoS and Medium range LoS) and using the 20 MHz channel in the more challenging scenarios (Long range NLoS and Long range mixed). We believe this demonstrates the different advantages of the PHY used in each network. Using the 80 MHz channel allows higher bit-rate and interference-robustness than 20 MHz channel. This leads to less re-transmissions for synchronization frames in good RF propagation conditions. However, the 20 MHz channel allows lower receiver sensitivity (i.e., higher link budget) than the 80 MHz channel. This allows it to deliver the synchronization frames with less re-transmissions in more challenging propagation environments (as in Long range NLoS and Long range mixed), provided the absence of interference.

4.3. ROS constrained delay ratio

We measure the CDR for ROS control packets that arrived with latency <75 ms.

We show the results in Table 2 for the network at steady state. We observe that the 6 GHz band resulted in the best performance in all locations. The wide 160 MHz channel was the best configuration

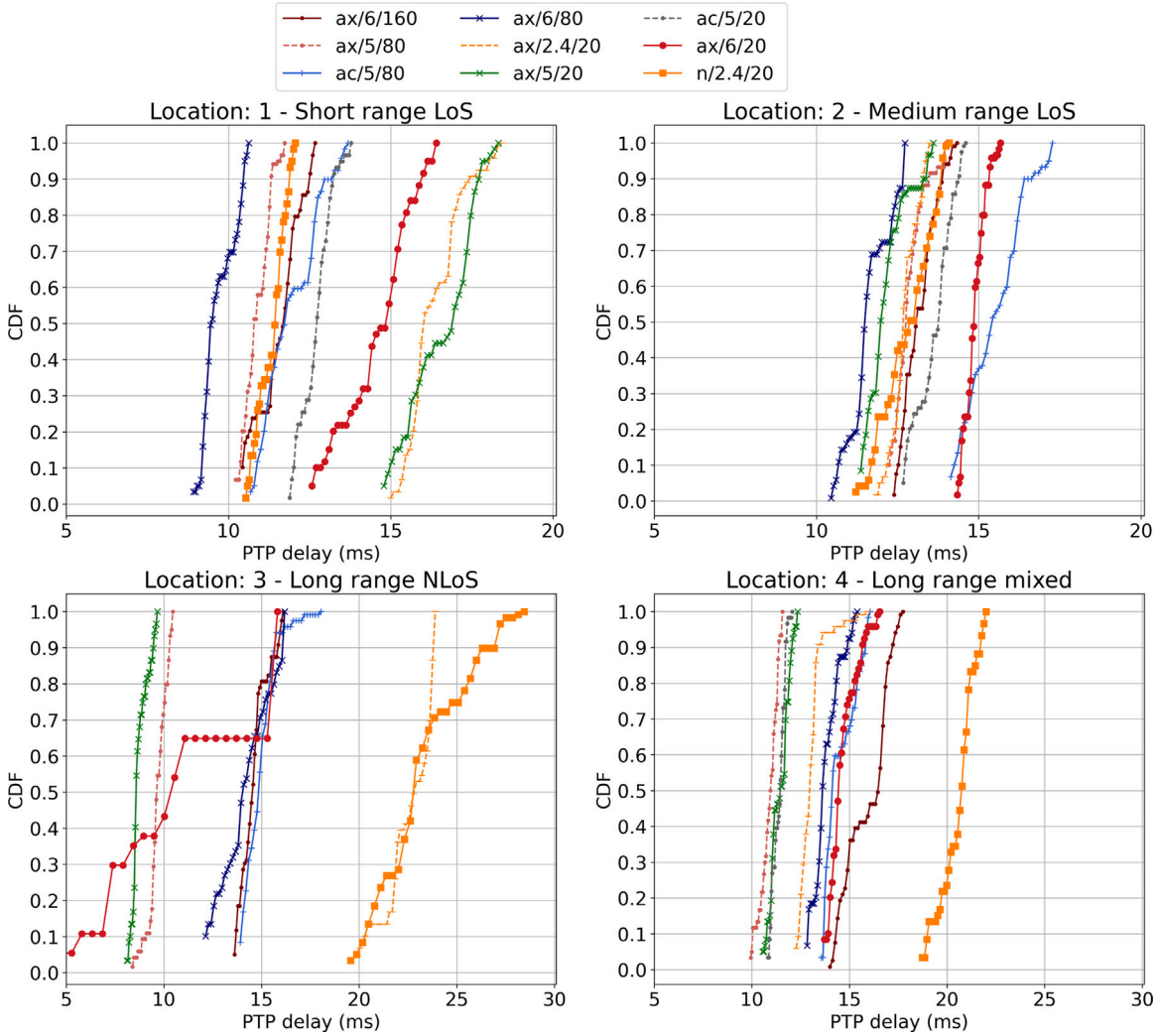

Fig. 9. CDF of PTP delay for each experiment (note: we use different x-axis ranges to improve plot readability).

for Short range LoS and Medium range LoS scenarios. In the Long range NLoS and Long range mixed scenarios, the best performance was achieved by 80 MHz an 20 MHz channel BW respectively. It is surprising that 6 GHz band would provide the highest control reliability in terms of CDR since it is expected to have shorter range than 5 GHz and 2.4 GHz bands. However, this can be attributed to the impact of interfering networks in the 2.4 GHz and 5 GHz bands as seen in the site RF scans (Figs. 4 and 5)

Similar to previous KPIs, we observe that the IEEE 802.11ax network did not always maintain better performance than older generations. For example, in the Short range LoS scenario, the ax/2.4/20 had the least CDR of all configurations. This confirms that using more recent Wi-Fi generations alone does not necessarily improve the network performance for control applications, specially in the presence of external interference.

But *how many of these overdelays happened successively?*. Knowing how often did overdelays happened back-to-back helps us evaluate the redundancy needed to increase the network reliability. We show in Fig. 11 a heat map of how many times packets were overdelayed successively. We see that a network can have up to 14 occurrences of 1 overdelay such as the ax/6/20 network in the Short range LoS scenario . Whereas in other networks, such as the n/2.4/20 network, had up to 4 successive overdelays in the same scenario. This indicates that packet overdelay may happen in isolated incidents or in bursts. We discuss in Section 6 possible mitigation techniques of this phenomena for future research.

4.4. Best performance highlights

We provide an overview of the best performing configuration in each location with respect to each KPI in Table 3. We observe three key conclusions.

First, there is not one configuration that is best for all KPIs. Therefore, there is need to adapt the used PHY configuration on a frame-by-frame basis based on the type of packet.

Second, all best performing configurations are in the 5 GHz and 6 GHz bands using Wi-Fi 6. This is a surprise because higher frequencies are expected to have lower link budget. This indicates that the interference in the 2.4 GHz band made it least performing (even for Wi-Fi 6), despite its higher link budget. We also note that most of the configurations use the 80 MHz and 160 MHz BW. This indicates the robustness of the wide-band channels against multi-path fading in metallic environments. But this comes at the cost of frequency band resource use.

Third, we note that the best configurations in terms of PTP delay are different form the best configurations for ROS delay. This is due to two reasons: (1) ROS uses application-level retries via DDS layer while PTP is uses native UDP as illustrated in Fig. 7. (2) ROS packets go through more layers of processing (DDS and RTPS) in addition to UDP/IP. Therefore, the end-to-end delay can suffer from additional overhead due to processing bottlenecks or buffer overflows. Therefore there is need to a PHY selection metric that considers the end-to-end delay for a more reliable performance.

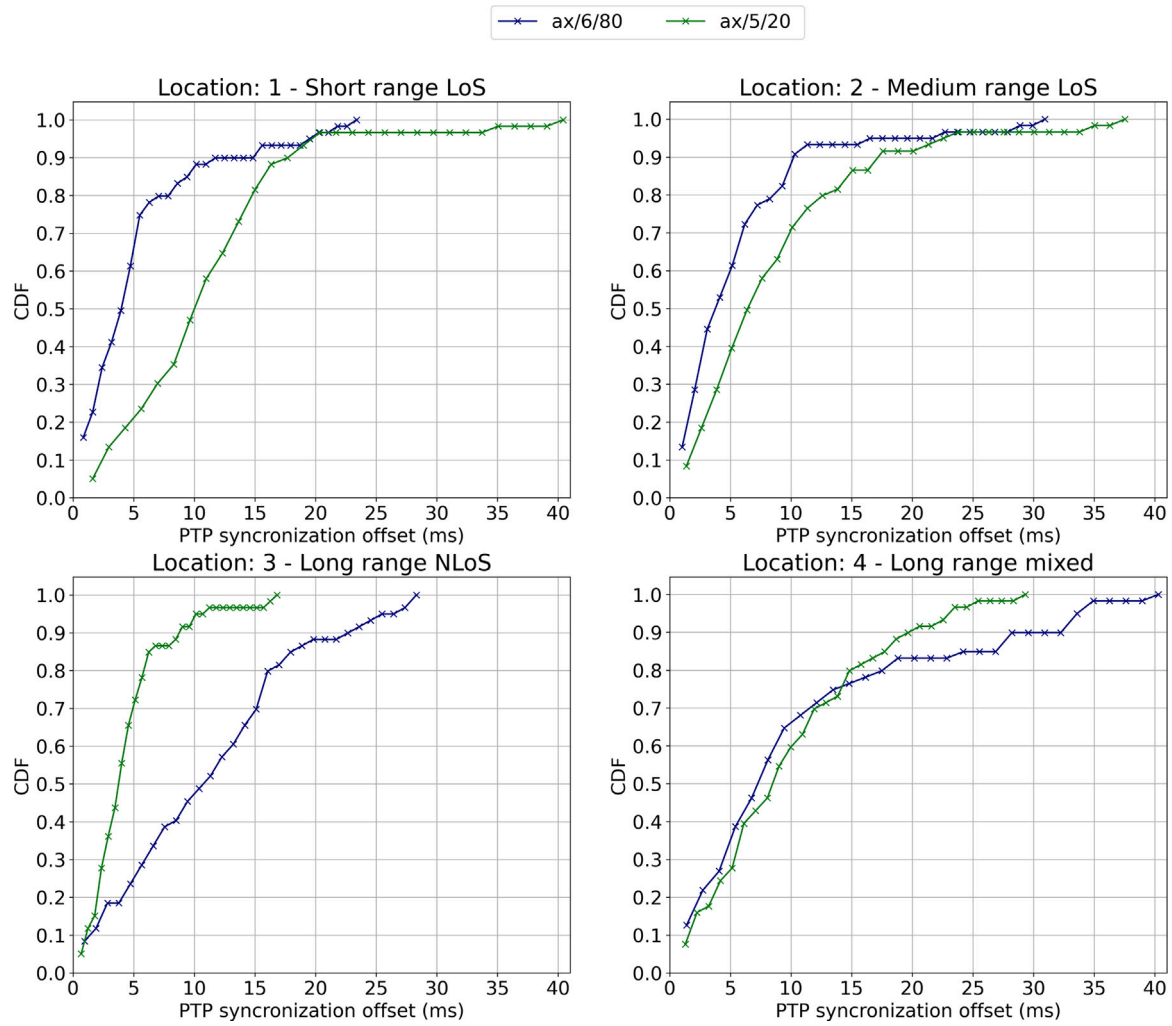

Fig. 10. CDF of PTP synchronization offset (in absolute value) for the best performing configurations.

Table 2
Constrained delay ratio for each configuration and location at steady state. Control packets delivered after delay >75 ms are considered detrimental for the teleoperator.

Configuration	Short range LoS	Medium range LoS	Long range NLoS	Long range mixed
ax/6/160	**94%**	**97%**	93%	92%
ax/5/80	89%	93%	98%	94%
ac/5/80	90%	90%	90%	93%
ax/6/80	91%	90%	**99%**	88%
ax/2.4/20	84%	93%	87%	94%
ax/5/20	91%	92%	98%	93%
ac/5/20	93%	91%	0%	93%
ax/6/20	87%	93%	49%	**95%**
n/2.4/20	90%	88%	83%	83%

Furthermore, *what is the performance trade-off between the configurations in each scenario?*. We show in Table 4 the relative performance degradation for each KPI for each configuration in the four scenarios. The best configuration is outlined in bold red in each KPI. It is calculated as the mean of the measurements in steady state in the after 120 s into the experiment. The rest of the values are presented as relative increase for PTP delay KPI or relative decrease for ROS CDR and throughput KPIs. Cell shading visualizes the best performing configuration.

Although there is no one configuration that is best for all KPIs in all scenarios, there can be reasonable compromises depending on application requirements. For example, in the Short range LoS and Medium range LoS scenarios, using ax/6/160 can be a reasonable compromise if the application can tolerate an additional mean delay of <2 ms in PTP exchanges. This motivates interest in a multi-PHY network where the STA can switch PHY on a frame-by-frame bases based on KPI objectives for each frame.

5. Lessons learned and research perspectives

Our experimental setup in an industrial shipyard and in the presence of interference, allowed us to test the limits of different Wi-Fi standards and configurations in a realistic environment. As we planned the experiment in such a complex site, we chose to run the experimental campaigns in four carefully selected locations instead of repeating the experiment in the same location. This allowed us to run tests across a mix of environmental characteristics and look for consistent patterns across locations.

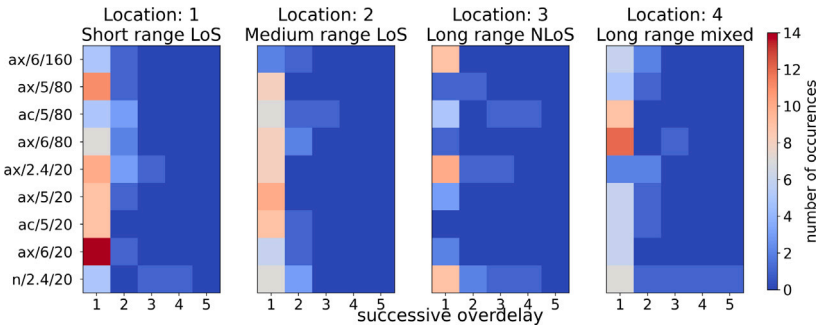

Fig. 11. Heatmap of the successive overdelays in each network. It indicates a potential for performance improvement using 2 redundant transmissions.

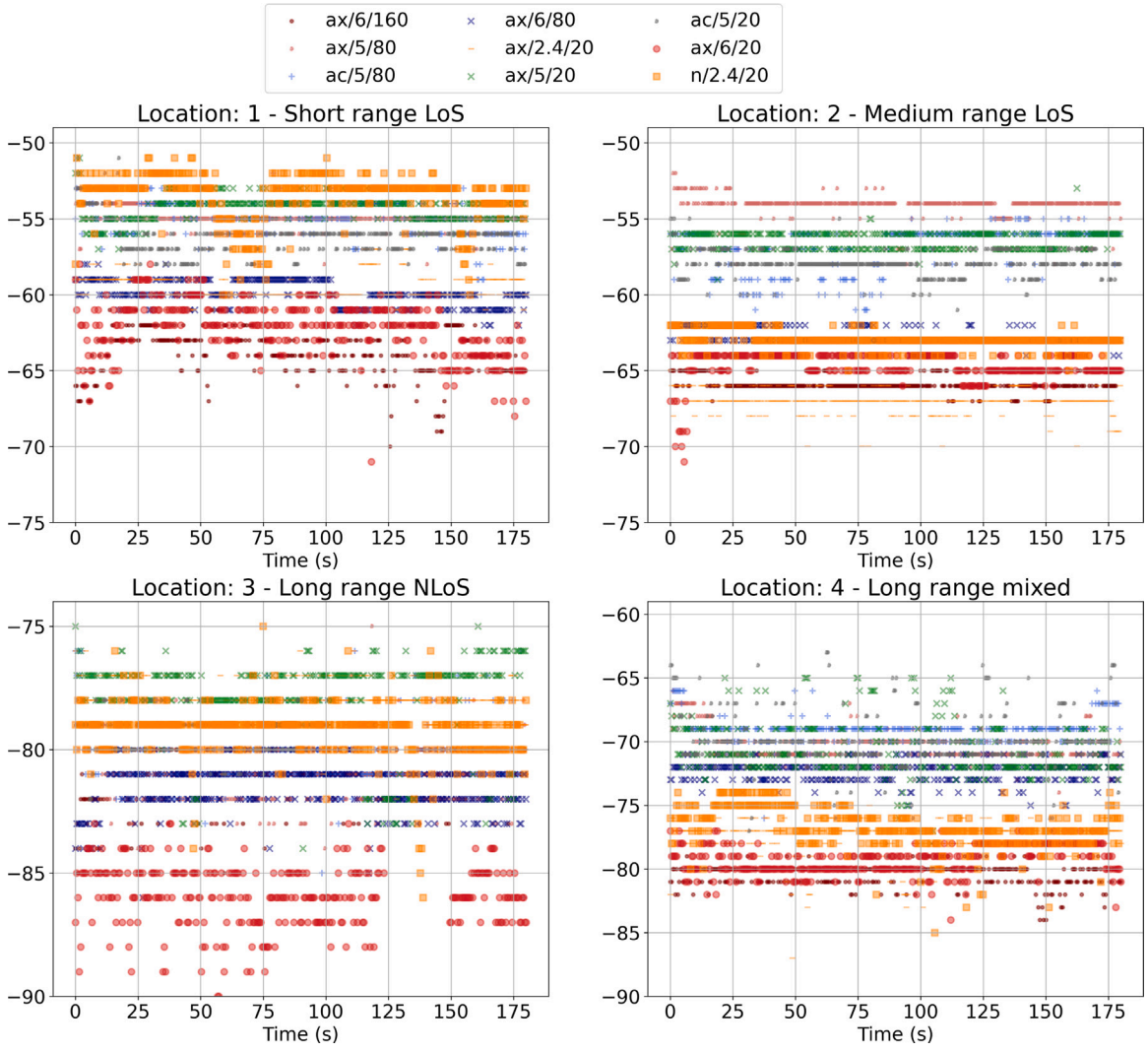

Fig. 12. Stable RSSI across each experiment reflects a relatively stable RF environment.

To assess the reliability of the results, we consider the stability of the propagation environment by looking at the variation of the link RSSI during each experiment. In Fig. 12, we show a scatter plot of the link RSSI for each configuration in each location. We observe that the RSSI for each configuration remains stable with ±2 dBm variation. Similarly, the used MCS is a key factor in the observed performance. We plot the used MCS in each Wi-Fi in Fig. 13. We notice that MCS was generally stable in most experiments, which reflects the stability of environment. Therefore, the physical conditions on site did not compromise the stability of the measurements.

While some of the obtained results might vary in another industrial outdoor scenarios, we believe that our findings are relevant and interesting to the research community. We distill below some important lessons that can be learned from our experiments.

Extensive logging and automation improve the reliability and speed of experimental campaign: As we had limited access to the shipyard, we maximized automation and the collected parameters. A timer-based shell script initiated sub-scripts to captured status parameters of PTP, WNIC, `iPerf`, ROS application, and AP scans. While we only report 6 parameters in this paper, we processed 240 files and we

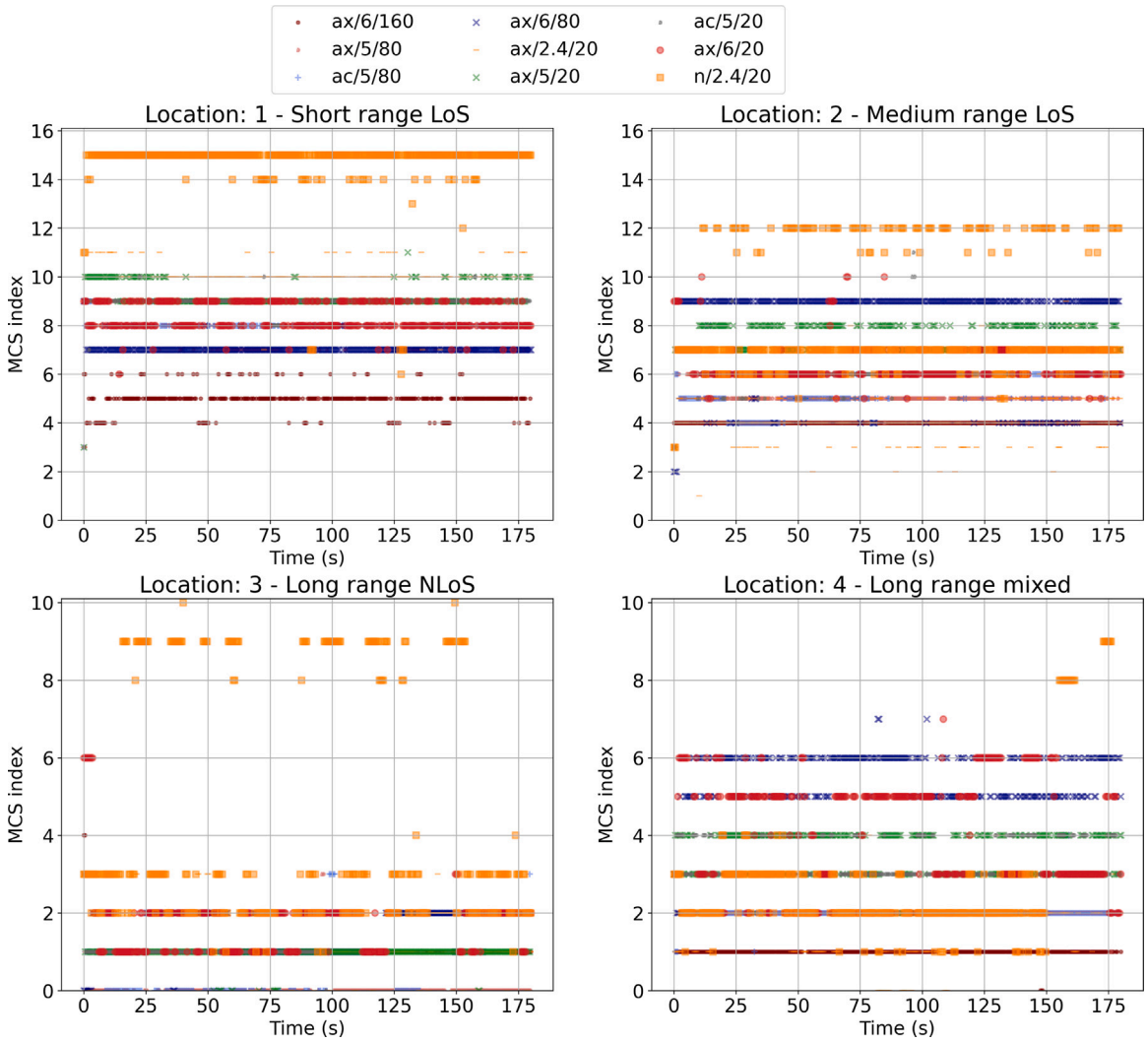

Fig. 13. Used MCS of each Wi-Fi configuration in the four locations during experiment runs.

Table 3
Summary of best performing configuration for each scenario and KPI. All best performing configurations are in the 5 and 6 GHz channels.

	PTP delay (Fig. 9)	ROS constrained delay (Table 2)	Throughput (Fig. 8)
Short range LoS (13 m)	ax/6/80	ax/6/160	ax/6/160
Medium range LoS (60 m)	ax/6/80	ax/6/160	ax/6/160
Long range NLoS (130 m)	ax/5/20	ax/6/80	ax/6/160
Long range mixed (150 m)	ax/5/80	ax/6/20	ax/6/80

extracted 56 parameters for each experimental run. This allowed us to do a posteriori investigation to understand the network behavior. For example, we were able to find instances where AP interference influenced the throughput and we ensured the correct execution of PTP engine and `iPerf`. We could also verify that the proper PHY configuration was used for each experiment through the collected WNIC reports.

Frequency diversity can be interesting for narrow-band OFDM: Presence of strong interference in the 2.4 GHz band proved limiting for OFDM performance in the 20 MHz band. We note that the ax/5/20 network had the same throughput as n/2.4/20 network, although it supports theoretical bit-rates twice as fast (Table 1). Configurations in the 5 GHz and 6 GHz bands achieved higher throughput using the same channel BW. We believe that a more dynamic channel adaptation is needed for the narrow-band OFDM due to its particular vulnerability to interference. Furthermore, the retry chains of the RAA may benefit from multi-band retries for narrow-band OFDM.

Optimizing for network latency can be independent from optimizing for throughput: As seen in Table 3, configurations with highest throughput are not the same as configurations with lowest PTP latency in all scenarios. This seems counter-intuitive as high end-to-end throughput means data is transferred faster. We believe that since throughput is measured by `iPerf` at 1 s intervals (the smallest configuration), it may not give an accurate idea of the distribution of this throughput across the 1 s period. We consider an example of two links L_{10} and L_{100} with measured end-to-end throughput of 10 Mbps and 100 Mbps respectively and that a packet of 100 B is to be transmitted on each link. Link L_{10} is uniformly transmitting at 1 Mb per 100 ms. However, link L_{100} achieves 100 Mbps by remaining idle for 500 ms and then transmitting at 200 Mbps for the remaining 500 ms. In this case, the packet is likely to experience delay <100 ms on link L_{10} and delay >500 ms on link L_{100}. Since the robotic network has critical latency requirement, the RAA needs to be aware of the latency of each rate. The main RAA implementations such as Minstrel (introduced in See. 2.1), focus only on throughput. More work can be done in this direction.

Table 4
Performance cost of selecting a configuration at each location.

Scenario	Short range LoS - 13 m			Medium range LoS - 60 m			Long range NLoS - 130 m			Long range mixed - 150 m		
Configuration/KPI	PTP Delay	ROS Delay <75 ms	Throughput	PTP Delay	ROS Delay <75 ms	Throughput	PTP Delay	ROS Delay <75 ms	Throughput	PTP Delay	ROS Delay <75 ms	Throughput
ax/6/160	+1.84 ms	94%	622 Mbps	+1.52 ms	97%	577 Mbps	+5.85 ms	-7%	89 Mbps	+5.02 ms	-3%	-107 Mbps
ax/5/80	+1.17 ms	-5%	-157 Mbps	+1.20 ms	-3%	-227 Mbps	+0.95 ms	-2%	-78 Mbps	10.87 ms	-1%	-63 Mbps
ac/5/80	+2.20 ms	-4%	-120 Mbps	+3.83 ms	-7%	-218 Mbps	+6.14 ms	-9%	-39 Mbps	+3.61 ms	-2%	-55 Mbps
ax/6/80	9.69 ms	-3%	-72 Mbps	11.62 ms	-7%	-235 Mbps	+5.42 ms	99%	-24 Mbps	+2.90 ms	-7%	187 Mbps
ax/2.4/20	+6.63 ms	-10%	-511 Mbps	+1.09 ms	-3%	-538 Mbps	+13.84 ms	-13%	-84 Mbps	+2.13 ms	-1%	-178 Mbps
ax/5/20	+6.84 ms	-3%	-473 Mbps	+0.49 ms	-5%	-464 Mbps	8.72 ms	-2%	-74 Mbps	+0.55 ms	-2%	-142 Mbps
ac/5/20	+2.99 ms	-2%	-482 Mbps	+1.99 ms	-6%	-472 Mbps				+0.50 ms	-2%	-144 Mbps
ax/6/20	+4.84 ms	-7%	-498 Mbps	+3.25 ms	-3%	-478 Mbps	+1.91 ms	-50%	-78 Mbps	+3.74 ms	95%	-145 Mbps
n/2.4/20	+1.63 ms	-4%	-549 Mbps	+1.17 ms	-8%	-542 Mbps	+14.36 ms	-17%	-85 Mbps	+9.66 ms	-13%	-184 Mbps

Latency requirement for an industrial robotic application is independent of raw link latency: The critical latency requirement of ROS control packets demands them to be delivered within a deadline of 75 ms. Therefore, if a link has consistent latency slightly less then 75 ms, it becomes more interesting than a link with much less latency than 75 ms with minor exceptions above 75 ms. As seen in Table 3, PHYs that are best for ROS application CDR are different from PHYs that are best for raw PTP delay. Moreover, we notice significant variation in ROS packet latency compared to PTP. To show this, we plot both delays in the time domain for the Short range LoS scenario in Fig. 14. Therefore, the application latency CDR requirement is an optimization objective that is independent from raw link latency. IEEE 802.11 QoS categories may possibly be extended to include such critical time requirements for small, low throughput, control packets.

Furthermore, future research can explore how redundancy can mitigate overdelay of control packets. A separate band or channel can be used to replicate control packets. Channel hopping for future Wi-Fi networks can be interesting to explore for mitigating the impact of interference on overdelay of control packets. Additionally, these techniques can be combined with use of IEEE 802.11 QoS categories to improve latency of critical control or synchronization packets.

6. Conclusion

In this paper, we evaluated the performance of Wi-Fi under nine different PHYs. We varied the frequency band, the channel bandwidth, and the maximum bit-rate. To mimic a classical scenario of industrial robotics, we installed PTP synchronization, streaming, and ROS control applications. The network was deployed in an industrial shipyard in the presence of high RF interference and metallic obstructions. We characterize the performance of each configuration in terms of three KPIs: Streaming throughput (measured by `iPerf`) Delay (measured by PTP), and CDR of control packets (measured by ROS application). The observations indicate that there is no one configuration that offers the best KPI performance in all scenarios.

We found that all best configurations belonged to either the 5 GHz or the 6 GHz bands. This was a surprise as the 2.4 GHz band is expected to higher robustness due to its lower frequency. We noted heavy interference in the industrial site that can explain the underperformance of the 2.4 GHz band. We note that configurations with higher channel BW performed best for streaming throughput but lower channel BW performed best for PTP delay. This was a surprise since throughput is a function of delay. This can be explained due to the fact the streaming application deployed end-to-end retries using TCP as opposed to the PTP application that used UDP . This indicates that high bit-rate configurations that use wide BW can offer better delay when using retries because of their small time-on-air. Finally, we noticed that in challenging scenarios such as NLOS or heavy metallic obstructions, there are wide trade-offs between the configurations. This can motivate switching between PHYs on a frame-by-frame basis depending on the objective KPI for each frame.

In future work, we address the challenges of deploying a Wi-Fi network in a swarm of robots in an industrial environment. Specifically, we target to propose rate adaptation algorithms that considers end-to-end KPIs such as: PTP delay or ROS CDR for control traffic.

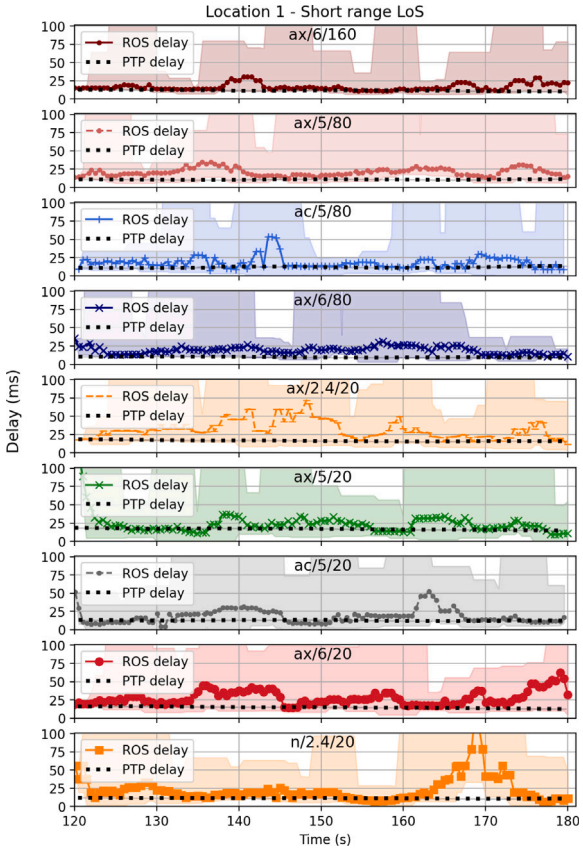

Fig. 14. ROS application delay and PTP path delay at steady state. The plot shows the simple moving median (5s window). Shaded region: `min` and `max` values.

CRediT authorship contribution statement

Mina Rady: Conceptualization, Data curation, Methodology, Project administration, Resources, Software, Writing – original draft, Writing – review & editing, Investigation, Supervision, Validation, Visualization. **Oana Iova:** Conceptualization, Funding acquisition, Methodology, Resources, Software, Supervision, Validation, Writing – original draft, Writing – review & editing, Data curation, Investigation, Project administration, Visualization. **Hervé Rivano:** Conceptualization, Funding acquisition, Investigation, Methodology, Project administration, Resources, Software, Supervision, Validation, Visualization, Writing – original draft, Writing – review & editing, Data curation. **Angeliki Deligianni:** Data curation, Funding acquisition, Investigation, Project administration, Resources, Writing – original draft, Writing – review & editing, Validation. **Leonidas Drikos:** Data curation, Funding acquisition, Investigation, Project administration, Resources, Writing – original draft, Writing – review & editing, Validation.

Declaration of competing interest

The authors declare that they have no known competing financial interests or personal relationships that could have appeared to influence the work reported in this paper.

Data availability

Data and code are shared on git repository referred to in the paper.

Acknowledgments

This project has received funding from the European Union's Horizon 2020 research and innovation program under grant agreement No 871260. This work was conducted while the first author was affiliated with INSA Lyon, Inria, CITI.

References

[1] V. Alexandropoulou, T. Johansson, K. Kontaxaki, A. Pastra, D. Dalaklis, Maritime remote inspection technology in hull survey & inspection: A synopsis of liability issues from a European Union context, J. Int. Marit. Saf. Environ. Aff. Shipp. 5 (4) (2021) 184–195, http://dx.doi.org/10.1080/25725084.2021.2006463.

[2] American Bureau of Shipping, ABS-49: guidance notes on the inspection, maintenance and application of marine coating systems, 2007.

[3] R.P. Rathiskumar, Quality inspection of vessel / ship without human involvement – current trends and future, 2022.

[4] F.M. Shah, T. Gaggero, M. Gaiotti, C.M. Rizzo, Condition assessment of ship structure using robot assisted 3D-reconstruction, Ship Technol. Res. 68 (3) (2021) 129–146, http://dx.doi.org/10.1080/09377255.2021.1872219.

[5] P. Sotiralis, K. Louzis, N.P. Ventikos, The role of ship inspections in maritime accidents: An analysis of risk using the bow-tie approach, Proc. Inst. Mech. Eng. O 233 (1) (2018) 58–70, http://dx.doi.org/10.1177/1748006x18776078.

[6] H. Huang, D. Li, Z. Xue, X. Chen, S. Liu, J. Leng, Y. Wei, Design and performance analysis of a tracked wall-climbing robot for ship inspection in shipbuilding, Ocean Eng. 131 (2017) 224–230, http://dx.doi.org/10.1016/j.oceaneng.2017.01.003.

[7] C. Bălan, The disruptive impact of future advanced ICTs on maritime transport: a systematic review, Supply Chain Manag.: Int. J. 25 (2) (2018) 157–175, http://dx.doi.org/10.1108/scm-03-2018-0133.

[8] R. Capocci, G. Dooly, E. Omerdić, J. Coleman, T. Newe, D. Toal, Inspection-class remotely operated Vehicles—A review, J. Mar. Sci. Eng. 5 (1) (2017) 13, http://dx.doi.org/10.3390/jmse5010013.

[9] D.L. McLean, M.J.G. Parsons, A.R. Gates, M.C. Benfield, T. Bond, D.J. Booth, M. Bunce, A.M. Fowler, E.S. Harvey, P.I. Macreadie, C.B. Pattiaratchi, S. Rouse, J.C. Partridge, P.G. Thomson, V.L.G. Todd, D.O.B. Jones, Enhancing the scientific value of industry Remotely Operated Vehicles (ROVs) in our oceans, Front. Mar. Sci. 7 (2020) http://dx.doi.org/10.3389/fmars.2020.00220.

[10] M.A. Hathibelagal, R.G. Garroppo, G. Nencioni, Experimental comparison of migration strategies for MEC-assisted 5G-V2X applications, Comput. Commun. 197 (2023) 1–11, http://dx.doi.org/10.1016/j.comcom.2022.10.009.

[11] S. Aggarwal, M. Ghoshal, P. Banerjee, D. Koutsonikolas, An experimental study of the performance of IEEE 802.11ad in smartphones, Comput. Commun. 169 (2021) 220–231, http://dx.doi.org/10.1016/j.comcom.2021.01.006.

[12] A.T. de Oliveira Filho, E. Freitas, P.R.X. do Carmo, D.H.J. Sadok, J. Kelner, An experimental investigation of Round-Trip Time and virtualization, Comput. Commun. 184 (2022) 73–85, http://dx.doi.org/10.1016/j.comcom.2021.12.006.

[13] IEEE, IEEE Standard for information technology— Telecommunications and information exchange between systems –Part 11: Wireless LAN Medium Access Control (MAC) and Physical Layer (PHY) specifications, 2016.

[14] IEEE, 802.11Ax-2021 - IEEE Standard for information technology–telecommunications and information exchange between systems local and metropolitan area networks–specific requirements part 11: Wireless LAN Medium Access Control (MAC) and Physical Layer (PHY) specifications amendment 1: Enhancements for high-efficiency WLAN, 2021.

[15] E. Khorov, A. Kiryanov, A. Lyakhov, G. Bianchi, A tutorial on IEEE 802.11ax high efficiency WLANs, IEEE Commun. Surv. Tutor. 21 (1) (2019) 197–216, http://dx.doi.org/10.1109/COMST.2018.2871099.

[16] E. Khorov, I. Levitsky, I.F. Akyildiz, Current status and directions of IEEE 802.11be, the future Wi-Fi 7, IEEE Access 8 (19659034) (2020) 88664–88688, http://dx.doi.org/10.1109/ACCESS.2020.2993448.

[17] I. Sammour, G. Chalhoub, Evaluation of rate adaptation algorithms in IEEE 802.11 networks, Electronics 9 (9) (2020) 1436, http://dx.doi.org/10.3390/electronics9091436.

[18] Minstrel rate control algorithm for mac80211, 2016, https://wireless.wiki.kernel.org/en/developers/documentation/mac80211/ratecontrol/minstrel, Accessed: 19 September, 2023.

[19] D. Xia, J. Hart, Q. Fu, On the performance of rate control algorithm Minstrel, in: 2012 IEEE 23rd International Symposium on Personal, Indoor and Mobile Radio Communications, PIMRC, IEEE, 2012, pp. 406–412, http://dx.doi.org/10.1109/pimrc.2012.6362819.

[20] S. Muhammad, J. Zhao, H. Refaim Hazem, An empirical analysis of IEEE 802.11 ax, in: 2020 International Conference on Communications, Signal Processing, and their Applications, ICCSPA, IEEE, 2021, pp. 1–6, http://dx.doi.org/10.1109/ICCSPA49915.2021.9385748.

[21] F. Frommel, G. Capdehourat, B. Rodriguez, Performance analysis of Wi-Fi networks based on IEEE 802.11ax and the coexistence with legacy IEEE 802.11n standard, in: 2021 IEEE URUCON, IEEE, 2021, pp. 492–495, http://dx.doi.org/10.1109/urucon53396.2021.9647207.

[22] F. Tramarin, A. K. Mok, S. Han, Real-time and reliable industrial control over wireless LANs: Algorithms, protocols, and future directions, Proc. IEEE 107 (6) (2019) 1027–1052, http://dx.doi.org/10.1109/jproc.2019.2913450.

[23] S. Hayat, E. Yanmaz, C. Bettstetter, Experimental analysis of multipoint-to-point UAV communications with IEEE 802.11n and 802.11ac, in: 2015 IEEE 26th Annual International Symposium on Personal, Indoor, and Mobile Radio Communications, PIMRC, IEEE, 2015, pp. 1991–1996, http://dx.doi.org/10.1109/pimrc.2015.7343625.

[24] IEEE 1588-2008 standard for a precision clock synchronization protocol for networked measurement and control systems, 2008, http://dx.doi.org/10.1109/ieeestd.2008.4579760.

[25] O. Seijo, I. Val, J.A. Lopez-Fernandez, M. Velez, IEEE 1588 clock synchronization performance over time-varying wireless channels, in: 2018 IEEE International Symposium on Precision Clock Synchronization for Measurement, Control, and Communication, ISPCS, IEEE, 2018, pp. 1–6, http://dx.doi.org/10.1109/ispcs.2018.8543078.

[26] M.-T. Thi, S. Guedon, S.B.H. Said, M. Boc, D. Miras, J.-B. Dore, M. Laugeois, X. Popon, B. Miscopein, IEEE 802.1 TSN time synchronization over Wi-Fi and 5G mobile networks, in: 2022 IEEE 96th Vehicular Technology Conference, VTC2022-Fall, IEEE, 2022, pp. 1–7, http://dx.doi.org/10.1109/vtc2022-fall57202.2022.10012852.

[27] S. Sudhakaran, K. Montgomery, M. Kashef, D. Cavalcanti, R. Candell, Wireless time sensitive networking for industrial collaborative robotic workcells, in: 2021 17th IEEE International Conference on Factory Communication Systems, WFCS, IEEE, 2021, pp. 91–94, http://dx.doi.org/10.1109/WFCS46889.2021.9483447.

[28] Object Management Group, The real-time publish-subscribe protocol (RTPS) DDS interoperability wire protocol specification, 2019, https://www.omg.org/spec/DDSI-RTPS/2.3.

[29] Object Management Group, OMG Data Distribution Service (DDS), 2015, http://www.omg.org/spec/DDS/1.4.

[30] ROS 2 documentation: Humble, 2023, https://docs.ros.org/en/humble/index.htm, Accessed: 16 March, 2023.

[31] P. Pandey, R. Parasuraman, Empirical analysis of Bi-directional Wi-Fi network performance on mobile robots in indoor environments, in: 2022 IEEE 95th Vehicular Technology Conference, VTC 2022-Spring, IEEE, 2022, 22013803, http://dx.doi.org/10.1109/vtc2022-spring54318.2022.9860438.

[32] R. Abu-Aisheh, F. Bronzino, M. Rifai, L. Salaun, T. Watteyne, Coordinating a swarm of micro-robots under lossy communication, in: Proceedings of the 19th ACM Conference on Embedded Networked Sensor Systems, ACM, 2021, pp. 635–641, http://dx.doi.org/10.1145/3485730.3494040.

[33] I.S. MacKenzie, A. Sellen, W.A.S. Buxton, A comparison of input devices in element pointing and dragging tasks, in: Proceedings of the SIGCHI Conference on Human Factors in Computing Systems Reaching Through Technology - CHI'91, ACM Press, 1991, pp. 161–166, http://dx.doi.org/10.1145/108844.108868.

[34] I.S. MacKenzie, C. Ware, Lag as a determinant of human performance in interactive systems, in: Proceedings of the SIGCHI Conference on Human Factors in Computing Systems - CHI'93, ACM, 1993, pp. 488–493, http://dx.doi.org/10.1145/169059.169431.

[35] Hellenic shipyards of Perama S.A., 2023, http://www.hsop.gr/, Accessed: 9 March, 2023.

[36] Asus, User manual: GT-AXE11000 ROG rapture tri-band gaming router, 2021.

[37] Ptpd - Precision Time Protocol daemon (1588-2008), 2023, https://manpages.ubuntu.com/manpages/xenial/man8/ptpd.8.html, Accessed: 19 July, 2023.

[38] iPerf - The ultimate speed test tool for TCP, UDP and SCTP, 2023, https://iperf.fr/, Accessed: 19 July, 2023.

[39] M. Allman, V. Paxson, E. Blanton, IETF RFC5681: TCP Congestion Control, IETF, 2009.

Mina Rady is a Research Engineer at the French Alternative Energies and Atomic Energy Commission in the area of Time Sensitive Networking. Previously, he was post-doctoral researcher at INSA Lyon where he contributed to this work. He received his Ph.D. in Computer Science from Sorbonne University, Paris, France in 2022. He held a simultaneous research and development engineer position at Orange Labs, France (former France Telecom). His experience includes: development of experimental evaluation of Wi-Fi for robotic systems, development of the IETF standard 6TiSCH protocol

stack for Industrial Internet of Things, distributed routing in RPL, and optimization solutions for low power wide area networks resource allocation.

Oana Iova is an associate professor at INSA Lyon, France since 2017. She received her Ph.D. in computer science from University of Strasbourg, France in 2014. Her research is in performance evaluation, routing and MAC protocols for wireless networks, with a focus on low-power long-range technologies for the Internet of Things.

Hervé Rivano is Full Professor at INSA Lyon and the head of the Inria/INSA Lyon common team Agora of the CITI lab which focuses on wireless networks in Smart Cities. He obtained his Ph.D. in November 2003 from the University of Nice-Sophia Antipolis and graduated from the Ecole Normale Supérieure de Lyon. His research interests include combinatorial optimization applied to network design and provisioning. He focuses on capacity/energy tradeoff for urban cellular and mesh networks design and low cost and dense wireless sensor networks for environmental sensing.

Angeliki Deligianni is a Ph.D. student at the National Technical University of Athens (NTUA), in the School of Mechanical Engineering. She holds a Diploma in Mechanical Engineering, with expertise in Industrial Management and Operational Research, and presented a diploma thesis entitled "Software Development Technologies for the Implementation of Urban Freight Transport Systems". Her academic interests revolve around the areas of Risk Management, Stakeholder Analysis, Management Information Systems, Project Management.

Leonidas A. Drikos is a Naval Architect and Mechanical Engineer, MSc., graduated from the National Technical University of Athens (NTUA). His experience includes many years as technical and general manager in consultancy and technical firms in the maritime field. Leonidas also holds an MSc., in Applied Economics and Strategic Finance. He is cofounder of Glafcos Marine which acts as strategic planner and managing director. Besides his relation with experimental testing (mainly, tank testing) and assistant researcher during his main five year course in university, he is the originator of the OptiNav and MINOAS concepts, and the technical coordinator of the so-called EU project.